Nuclear Data Measuring Activities

i n

Japan

July, 1965

Japanese Nuclear Data Committee

Nuclear Data Measuring Activities in Japan

CONTENTS

July, 1965

Japanese Nuclear Data Committee

I. JAERI Reactor-Neutron Experiment Group

1. Automatic Data Recording System*

(Y.Ohno, T.Asami, K.Okamoto and K.Ideno)

An automatic data recording system for the experimental data treatment has been introduced to the JAERI neutron crystal monochromator. This system is able to punch out all measuring informations successively on a paper-tape of eight bits, which are the Bragg angles, sample numbers and counting rate for the "on"- or "off"-Bragg condition at either setting of the samples "in" and "out" of the neutron beam. The punched tape is then processed by an electronic computer for the calculations of the neutron total cross sections.

2. Measurements of Higher Order Contaminations**

(Y.Ohno, T.Asami, K.Okamoto and K.Ideno)

The problem of higher order contamination in monochromating neutrons by Bragg reflection from LiF(200) and (111) planes has been investigated. The higher order contaminations were examined with the transmission method applied for the foils of gold, and plates of boron glass.

---

*) A detailed description of this work will be published somewhere.

**) This work will be given in a JAERI publication.

3. Neutron Total Cross Sections of Some Rare Earth Element

(Y.Ohno, T.Asami, K.Okamoto and K.Ideno)

The total cross sections of Er, Dy, Eu and Eu^{151} have been measured by transmission method with the JAERI crystal monochromator and mechanical monochromator installed in reactors JRR-2 (10 MW) and JRR-1 (50 kW) respectively, in the neutron energies between 0.0005 and 0.05 eV. The rare earth elements were filled in a precision quartz case as the DNO_3-D_2O solution of their oxides. The results are given in the figures (See pp.4 and 5). The cross section measurements of enriched Gd and Sm samples are now being carried on for analysis of low energy resonances.

4. Comparison of Reactor-Neutron Absorption

(S.Otomo, Y.Ohno and T.Fuketa)

The reactor-neutron absorption effect of fifteen test samples of berylium oxide (2 cm dia. x 6 cm) was compared to each other by using the paired-chamber-type pile oscillator* at the reactor JRR-1. The neutron absorption effect was given in ppm of natural boron equivalent ΔX relative to one of the samples (reference sample) which was defined by the following formula:

$$\Delta X = \frac{(\Sigma_a/\rho \text{ of a sample}) - (\Sigma_a/\rho \text{ of the reference sample})}{\Sigma_a/\rho \text{ of natural boron}} \times 10^6,$$

---

*) T.Fuketa: Nucl. Instr. Methods 13, 35 (1961)

T.Fuketa, M.Ishii and S.Otomo: Pile Neutron Research in Physics, p.633, IAEA (1962)

where $\Sigma a/\rho$ means average neutron absorption cross section per unit mass for the neutron spectrum at the pile-oscillator detector. The experimental error for the value of ΔX ranged 0.2~0.7 ppm.

5. Preliminary Test of a Method of Measuring Large Neutron Dose

(S.Otomo and T.Fuketa)

A preliminary experiment has been performed to test feasibility of a method proposed for measuring large neutron dose.* The method is based on the following idea. The neutron absorption cross sections of some nuclides such as Gd^{157} and Cd^{113} are so large that irradiation of a sample containing such a nuclide under a high neutron flux will result in an appreciable decrease in the macroscopic neutron absorption cross section of the sample. The pile oscillator is a good instrument to measure such a change in the macroscopic cross section of the sample, and the irradiated neutron dose can be deduced from a relative measurement of the cross section of the sample before and after the irradiation. The result of the preliminary experiment met the expectation of the propose method, and main practical problem seems to consist in making an uniform thin sample which possesses low residual activity and reasonable mechanical strength after a great deal of irradiation.

---

*) T.Fuketa: Nucl. Sci. Engg., 13, 61 (1962)

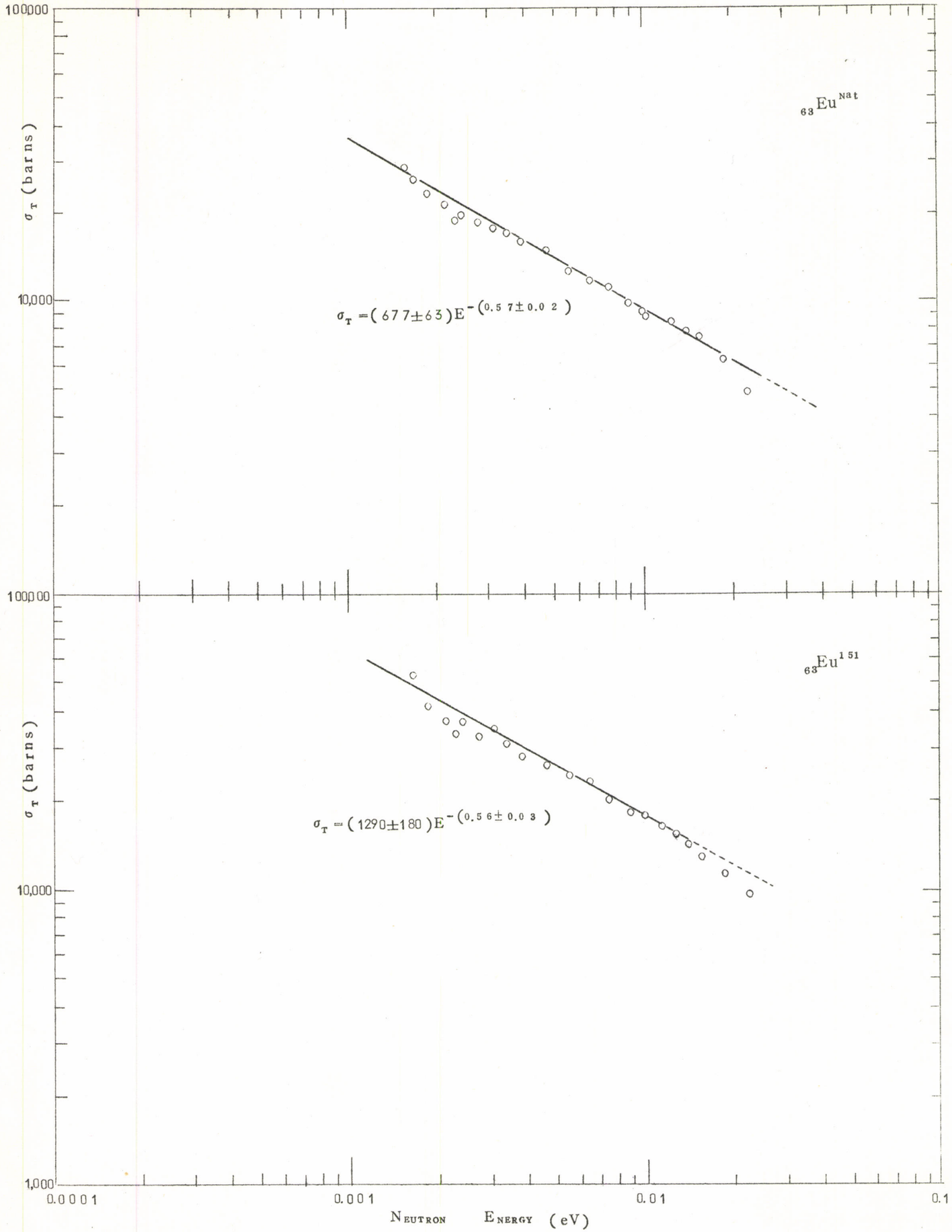
100000
10,000
1000 00
σ_T (barns)
$_{63}Eu^{Nat}$
$\sigma_T = (677 \pm 63) E^{-(0.57 \pm 0.02)}$
$_{63}Eu^{151}$
$\sigma_T = (1290 \pm 180) E^{-(0.56 \pm 0.03)}$
10,000
1,000
0.0001
0.001
0.01
0.1
NEUTRON ENERGY (eV)

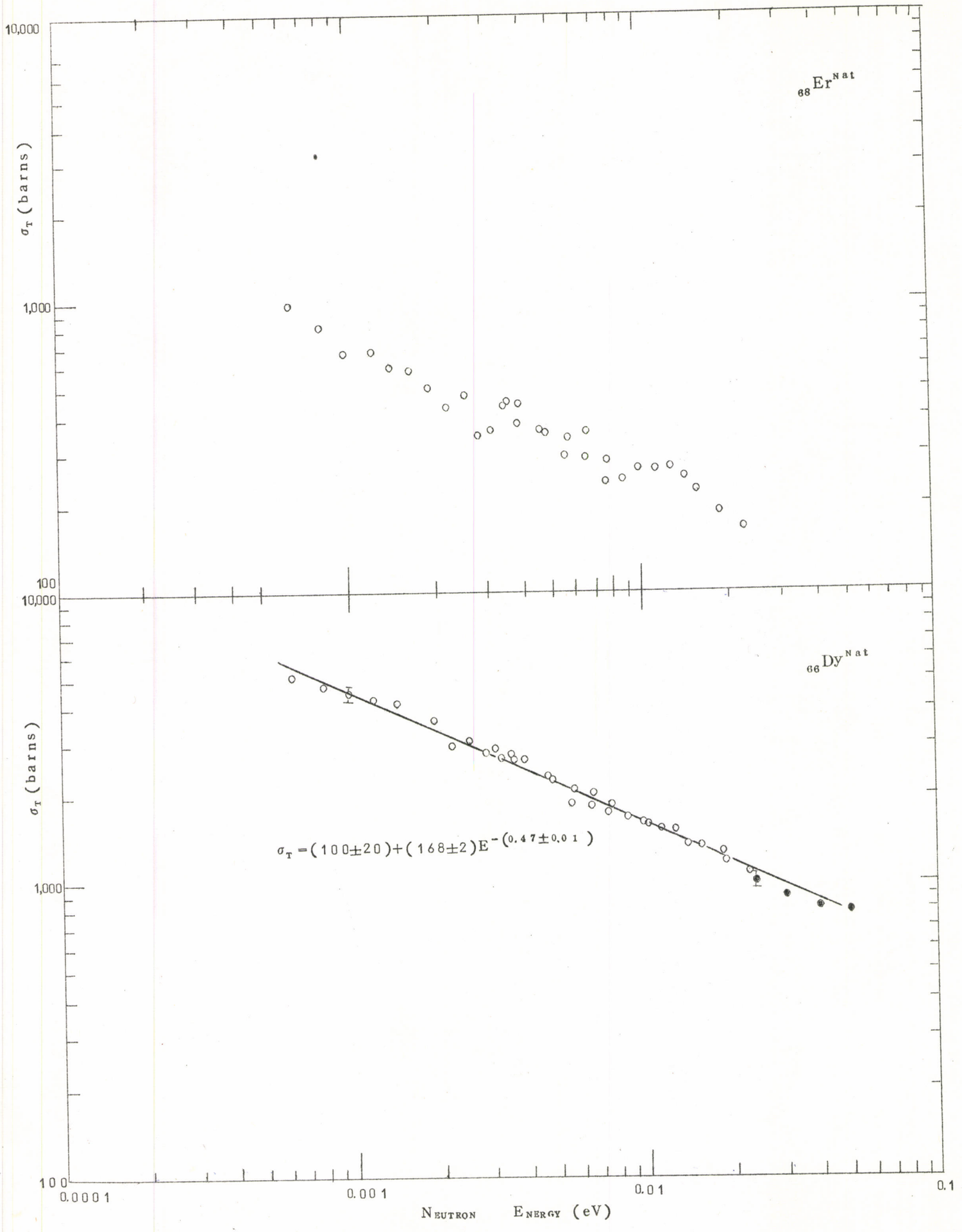
10,000
1,000
100
σ_T (barns)
$_{68}Er^{Nat}$
10,000
1,000
100
σ_T (barns)
$_{66}Dy^{Nat}$
$\sigma_T = (100 \pm 20) + (168 \pm 2) E^{-(0.47 \pm 0.01)}$
0.0001
0.001
0.01
0.1
NEUTRON ENERGY (eV)

II. JAERI Linac Group

1. Investigation of the Resolution Function of the Neutron Spectrometer

(H.Takekoshi, A.Asami, Y.Kawarasaki, M.Ohkubo and Y.Nakajima)

Calculations of the resolution function of the JAERI Linac time-of-flight spectrometer have been attempted assuming a few types of resolution function and using the well-known resonance parameters of tungsten and the measured transmission data. The widths of the resolution function obtained were found to be reasonable to the width calculated from the spectrometer characteristics, such as the neutron burst width and the channel width of the time analyzer.

2. Investigation of Capture Gamma Rays*

(Y.Kawarasaki)

The low energy gamma ray spectra following the neutron resonance captures have been measured with a crystal scintillation spectrometer (NaI(Tl), 3"ø x 3"), using the JAERI 20-MeV Linac and the time-of-flight techniques. The results hitherto obtained are shown in the following tables:

---

*) The details of the present investigation are given in JAERI 1073 (1965).

Table

In the first column of this table, the sample nuclide, natural abundance in %, the chemical form of the sample and its thickness are denoted. The second column contains the neutron resonance energy in eV, spin of the compound state, if known, and the gate-time adopted in this measurement, E_γ and I_γ in the third and fourth columns are the γ-ray energies in keV and their relative intensities obtained in this work, respectively.

Nuclide (Abundance) form	E_0(eV) Spin (Gate)	This work	
		E_γ(keV)	I_γ
$^{107}_{47}Ag$ (51.35) metalic plate 0.2 mmt	16.6 J = (170 ~ 190 μ sec)	85	85
		120	4
		140	5
		210	100
		260	7
		305	30
		760	20
$^{109}_{47}Ag$ (48.65) metalic plate 0.2 mmt	5.2 J = 1 (260 ~ 380 μ sec)	78	27
		122	44
		208	100
		245	64
		365	21
		380	19
		525	42
		740	5
$^{113}_{48}Cd$ (12.26) metalic plate 0.5 mmt	0.175 J = 1 (1.2 ~ 1.4 msec)	430	2
		558	100
		655	5
		790	4

- cont'd

Nuclide (Abundance) form	E_0(eV) Spin (Gate)	This work	
		E_γ(keV)	I_γ
$^{113}_{49}In$ (4.28) metalic plate 0.2 mmt	14.7 J = (184 ~ 192 μsec)	92	84
		130	100
		165	42
		285	14
		305	22
		395	15
		473	22
		535	24
$^{115}_{49}In$ (95.77) metalic plate 0.2 mmt	1.46 J = 5 (500 ~ 700 μsec)	65	34
		95	100
		188	81
		280	100
		335	10
		390	13
		425	6
		530	25
$^{115}_{49}In$ (95.77) metalic plate 0.2 mmt	3.86 J = 4 (340 ~ 380 μsec)	65	32
		95	88
		145	13
		188	63
		235	8
		280	100
		375	10
		400	10
		415	16
		530	26

- cont'd

Nuclide (Abundance) form	E_0(eV) Spin (Gate)	This work	
		E_γ(keV)	I_γ
$^{115}_{49}In$ (95.77) metalic plate 0.2 mmt	9.1 J = 5 (230 ~ 250 μsec)	65	35
		95	82
		145	16
		188	87
		280	100
		335	13
		375	9
		400	16
		530	20
$^{121}_{51}Sb$ (57.25) metalic grain 0.25 gr/cm^2	6.25 J = (270 ~ 300 μsec)	80	55
		125	100
		150	50
		225	12
		280	50
		445	20
$^{121}_{51}Sb$ (57.25) metalic grain 0.25 gr/cm^2	15.6 J = (170 ~ 190 μsec)	80	69
		125	100
		150	32
		225	7
		280	51
$^{123}_{51}Sb$ (42.75) metalic grain 0.25 gr/cm^2	21.6 J = (148 ~ 165 μsec)	90	100
		150	95
		270	34
		320	22
		400	13
		465	12

- cont'd

Nuclide (Abundance) form	E_0(eV) Spin (Gate)	This work	
		E_γ(keV)	I_γ
$^{147}_{62}Sm$ (14.97) oxide 25 mgr/cm^2	3.4 J = (380 ~ 400 μsec)	30	
		80	9
		150	13
		195	9
		340	23
		550	100
		620	35
$^{149}_{62}Sm$ (13.83) oxide 25 mgr/cm^2	0.096 J = 4 (1.9 ~ 2.5 msec)	340	100
		440	56
		570	8
		710	12
$^{149}_{62}Sm$ (13.83) oxide 25 mgr/cm^2	0.89 J = (700 ~ 800 μsec)	340	100
		440	56
		570	4
		680	7
		710	8
$^{152}_{62}Sm$ (26.72) oxide 25 mgr/cm^2	8.2 J = (240 ~ 260 μsec)	35	partially x-ray
		85	23
		135	100
		182	30
		415	42
		475	33
		560	18
		790	27
$^{151}_{63}Eu$ (47.82) oxide 13 mgr/cm^2	0.46 J = (850 ~ 1150 μsec)	40	x-ray
		90	

- cont'd

Nuclide (Abundance) form	E_0(eV) Spin (Gate)	This work	
		E_γ(keV)	I_γ
$^{162}_{66}Dy$ (25.53) oxide 13 mgr/cm^2	5.5 J = 1/2 (290 ~ 320 μsec)	45	x-ray
		78	33
		175	17
		265	25
		365	100
		410	55
$^{163}_{66}Dy$ (24.97) oxide 13 mgr/cm^2	1.7 J = (520 ~ 570 μsec)	45	x-ray
		75	100
		120	7
		180	68
		220	24
		275	18
		295	18
		420	18
		480	22
		675	25
		740	38
$_{68}Er$ oxide 28 mgr/cm^2	0.46 J = (1.0 ~ 1.1 msec)	48	x-ray
		80	18
		188	100
		285	10
		780	22
$_{68}Er$ oxide 38 mgr/cm^2	0.58 J = (880 ~ 960 μsec)	48	x-ray
		80	20
		188	100
		285	16
		780	27

- cont'd

Nuclide (Abundance) form	E_0(eV) Spin (Gate)	This work	
		E_γ(keV)	I_γ
$^{169}_{69}Tm$ (100) oxide 13 mgr/cm^2	3.9 J = (320 ~ 400 μsec)	50 120 160 215 320	x-ray 19 100 95 33
$^{177}_{72}Hf$ (18.5) oxide 38 mgr/cm^2	1.1 J = (620 ~ 720 μsec)	55 95 220 325 1150	x-ray 53 100 11 10
$^{178}_{72}Hf$ (27.1) oxide 38 mgr/cm^2	7.8 J = 1/2 (250 ~ 262 μsec)	55 115 165 220 320	x-ray 11 5 100 37
$^{181}_{73}Ta$ (99.9877) metalic grain 0.25 gr/cm^2	4.8 J = 4 (300 ~ 400 μsec)	57 135 175 275 405	x-ray 54 55 100 27
$^{195}_{78}Pt$ (33.8) metalic plate 0.05 mmt	12.0 J = 1 (190 ~ 230 μsec)	65 330 355	x-ray 76 100
$^{197}_{79}Au$ (100) metalic plate 0.1 mmt	4.9 J = 2 (300 ~ 400 μsec)	65 180 215 245 440	x-ray 62 100 96 8

3. Resonance Parameters of Co^{59}

(H.Takekoshi, A.Asami, Y.Kawarasaki, M.Ohkubo and Y.Nakajima)

The transmission measurements of the neutrons for the metalic cobalt samples of several thickness were performed with 20 ns/m resolution of neutron time-of-flight spectrometer. The data was analyzed for 132 eV resonance of Co^{59}, and following parameters were obtained by the area- and shape-analysis methods:

$$E_o = 132 \text{ eV},$$
$$\Gamma_{total} = 6.20 \pm 0.20 \text{ eV},$$
$$2g\Gamma_n = 5.76 \pm 0.10 \text{ eV},$$
$$\Gamma_n = 5.12 \pm 0.09 \text{ eV},$$
$$J = 4.$$

The results are in agreement with the parameters found in current literature within the accuracy attained.

4. Neutron Transmission Measurements on Cadmium

(H.Takekoshi, T.Fuketa, A.Asami, Y.Kawarasaki, M.Ohkubo and Y.Nakajima)

Neutron transmission measurements on natural cadmium samples by JAERI Linac Time-of-Flight Spectrometer with 50-m flight path are now in progress. Li-6 glass scintillators are used as neutron detectors, and neutron signals from the detectors are stored in a 4096-Channel TMC Time Analyzer. The whole measurements will cover the neutron energy range of up to a few keV with minimum resolution of about 10 ns/m for several sample thicknesses. Typical raw data of the "sample-in" counts for natural cadmium sample (99.999 per cent nominal purity) of 30-mm thickness are shown in the following figure. In the figure, several arrows show the resonances whose

energies are not listed in BNL-325 (2nd Edition)[1] but which were isotopically identified in the capture gamma-ray measurements by H.E. Jackson and L.M. Bollinger[2]. The analysis of the resonance dips by the area method will be carried out to get the resonance parameters.

---

1) D.J. Hughes and R.B. Schwartz: BNL-325 2nd Ed. (1958)

2) H.E. Jackson and L.M. Bollinger: Phys. Rev. 124, 1142 (1961)

FIGURE A Typical Raw Data of "Sample-In" Counts for Natural Cadmium Sample of 30-mm Thickness. The pictures were taken from the oscilloscope display of a part of the data in the 4096-channel analyzer. The resolution of the data was about 20 nanosec/m.

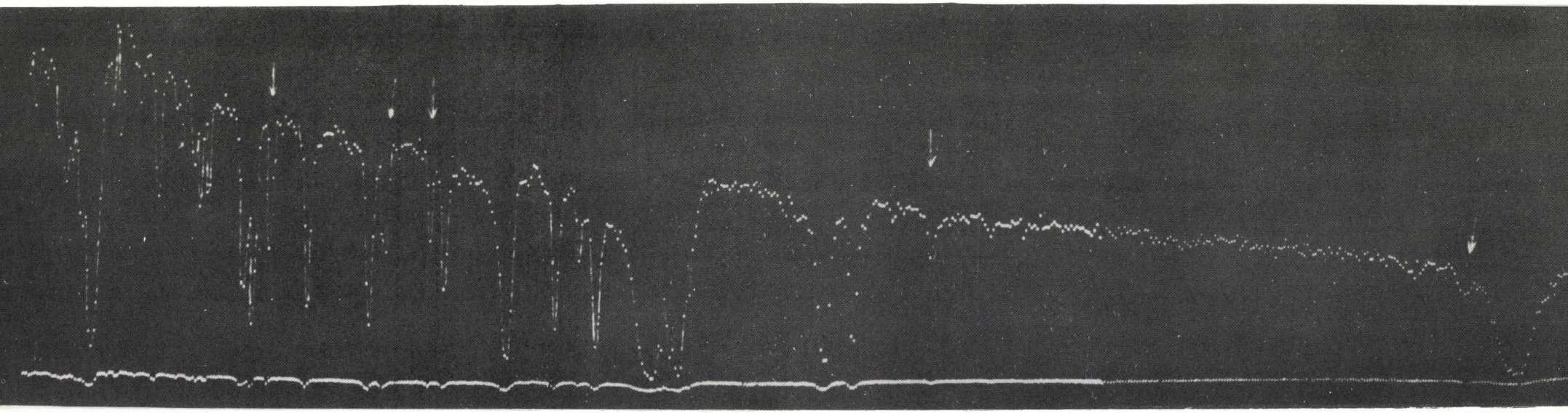

III. JAERI Van de Graaff Accelerators Group

1. Energy Dependence of the Nuclear Level Density at an Excitation below the Neutron-Binding Energy*

(K.Tsukada, S.Tanaka, M.Maruyama and Y.Tomita)

The energy spectra of neutrons inelastically scattered from Co, Ag, In, Ta, and Au have been measured in an energy range of 3.5 - 8.5 MeV (every 0.5 MeV step) of incident neutrons by means of the time-of-flight technique with pulsed-beam Van de Graaff accelerators and an ion buncher of Mobley type. The relations between the level density and the excitation energy are obtained in a range of 2 - 8 MeV. The inverse compound-formation cross sections for several forms of the optical-model potential are used in the derivation. For Co and Ag, the relations agree with the prediction of the Fermi-gas model. For In, Ta, and Au, there are obvious breaks in the observed relations at 4 - 5 MeV of the excitation. Below the breaks the observed points fit to the curves calculated by the constant-temperature model. Above the breaks they fit to those based on the Fermi-gas or constant-temperature model.

2. Average Level Width of the Compound Nucleus**

(K.Tuskada and J.Lee)

The ratio of average level width to average level spacing of the

---

*) This work will be published in the J. Phys. Soc. Japan.

**) Preliminary result has been reported in the Phys. Letters 11, 141 (1964). Details will be published somewhere.

compound nucleus in a strongly-overlapping-resonance region has been obtained by the self-indication measurement of the fluctuations in the neutron total cross sections. The observed ratios for Al, Si, and S with the excitation energy of 11 - 13 MeV are explained in terms of the strong-interaction model of the compound-formation process, though the observed values for Mn, Fe, Ni, Co, Cu, and Zn are systematically smaller than the calculated ones. The fluctuation in the excitation function of the nuclear reaction is analyzed under the condition that the energy resolution or the energy step of the measurement is much larger than the average total width and spacing of the compound states. An apparent period of the fluctuation and a width of the energy-correlation function of the cross sections are obtained as functions of the resolution or the energy step. As the results of the present analyses, it is pointed out that the average level width of the compound nucleus is not necessarily larger than the one predicted by the above-mentioned simple model of the compound process.

3. Directional Anisotropy in the Characteristics of the Organic-Crystal Scintillators II*

(K.Tsukada, S.Kikuchi and Y.Miyagawa)

The directional anisotropy in the scintillation response of anthracene and p-terphenyl crystals for fast neutrons has been measured in an energy range of 0.3 to 16 MeV. The anisotropy appears to have close correlations with directions of the molecular long axes (or the optical principal Z-axis), and the crystallographic

*) Details will be given in the Nucl. Inst. and Method.

b-axis. For the anthracene crystal, the molecular long axes correspond to the maximum scintillation response, though the direction of the maximum response changes with the neutron energy by about 30° in the above energy range, and the b-axis to the minimum response. For the p-terphenyl crystal, the direction of the molecular long axes coincides approximately with that of the minimum response, and the optical principal X-axis, which is perpendicular to both of the molecular axes and b-axis, coincides with the direction of the maximum response. An analysis for the energy dependence of the directional anisotropy of the anthracene crystal shows that the anomalous response can be explained by directional variations of the quenching term $B\frac{dE}{dx}$ in the formula proposed by Birks, that is, $\frac{dS}{dx} = A\frac{dE}{dx}\Big/(1 + B\frac{dE}{dx})$. The maximum variation of the quenching term amounts to 40 %.

4. The (p,n) Threshold Measurements on Fe^{57}, Cu^{65} and Se^{80}

(K.Nishimura, K.Okano and S.Kikuchi)

The (p,n) reaction threshold for Fe^{57} has been measured using the enriched isotope. The threshold energy obtained is consistent with the previous (p,n) measurements*). The Q-values from these measurements indicate that the adjusted mass difference of

---

*) A.J. Elwyn, H.H. Landon, S. Oleksa, and G.N. Glasoe : Phys. Rev. 112, 1200 (1958)

C.H. Johnson, C.C. Trail, and A. Galonsky : Phys. Rev. 136 B1719 (1964)

0.57 MeV*) between the grand states of Fe^{57} and Co^{57} is in error. The (p,n) thresholds for Cu^{65} and Se^{80} have also been measured precisely using thin targets, and the results obtained are consistent with our previous values**). The proton beam energy has been carefully calibrated by the (p,n) reactions on Li^7, C^{13}, and F^{19}.

5. The Be^9 (He^3, n)C^{11} Reaction

(K.Okano, S.Kikuchi and K.Nishimura)

The angular distributions of neutrons from the $Be^9(He^3, n)C^{11}$ reaction have been measured at four incident He^3 energies of 4.00, 4.49, 5.01 and 5.49 MeV. Neutron groups leading to the ground and first excited states of C^{11} were detected by a γ-suppressed stilben crystal of 2-inch diameter and 2-inch thickness. Excitation curves have also been measured from 3.5 to 5.5 MeV in 10-keV intervale. The angular distribution of a neutron group leading to the $3/2^-$ ground state of C^{11} could be fitted by the L = 0 stripping pattern of two nucleon stripping theory. The neutron group leading to the first excited state of C^{11}, however, does not show the expected L = 2 stripping pattern. The absolute differential cross sections obtained are considerably smaller than those recently obtained at Rice University***). Further study is now under way to extend the energy range by using doubly charged He^3 beams. Further (He^3, n)-reaction study is also planned on several elements such as Li^7, B^{11}, O^{16} and Ca^{40}.

---

*) F. Everling, L.A. König, J.H.E. Mattauch, and A.H. Wapstra : Nucl. Phys. 15, 342 (1960)

**) K.Okano and K.Nishimura : J. Phys. Soc. Japan : 18, 1563 (1963)

***) G.U.Din, J.L.Weil, and G.C. Phillips : ANL 6848, p.199

6. Studies of Excitation Cross Sections of $(n,n'\gamma)$ Reactions

(K.Nishimura, K.Okano and S.Kikuchi)

The cross sections of the $(n,n'\gamma)$ reactions of Fe, Co, Ni, Cu, Zn, Mo, Ag, Cd, and Sn have been measured in the energy range from 0.3 to 2.6 MeV, using a ring-geometry arrangement. The excitation curves obtained on the low-lying levels of these nuclides are presented. The excitation curves of Ni, Zn, Mo, Ag, and Sn are compared with the results of optical-model calculations based on the statistical model of Hauser and Feshbach. The transmission coefficients used in the calculations are those derived from the optical model potentials as proposed by Beyster, Emmerich, Bjorklund and Fernbach, Perey and Buck, and Sugie. The calculated cross sections are appreciably larger than the experimental values, except for the case of molybdenum. The calculated cross sections based on the Moldauer theory are also compared with the excitation curves of Ni, Zn, Mo, and Sn. In most cases, the results of the calculations by the Moldauer theory are in better agreement with the experimental ones than those of the Hauser-Freshbach calculations.

7. 5.5-MeV Ion Buncher of Mobley Type*

(K.Tsukada, S.Tanaka, M.Maruyama and Y.Tomita)

An ion buncher of Mobley type, a system for producing ion bursts of high intensity and of nanosecond duration, has been constructed for proton and deuteron beams from a 5.5-MV Van de Graaff accelerator, and has been successfully used for fast-neutron time-of-flight experiments. In the system an rf resonator is employed

---

*) Details will be given in the Nucl. Inst. and Method.

in order to obtain a high voltage (50 kV) of 24 Mc which should be supplied to the deflector. The Mobley magnet has a mass-energy product of 17. Bunched pulses of 1.0 ~2.8 ns duration at the target for proton and deuteron beams with energies of 2~5.5 MeV were observed on a sampling oscilloscope. The bunching ratio larger than 10 was obtained for the proton pulses of energies higher than 3 MeV and for the deuteron higher than 4 MeV. It was found that the inherent beam spread was almost cancelled out at the target by the linear-acceleration effect which was caused by the change in potential between the deflector plates.

IV. Tokyo Institute of Technology Group (Research Laboratory of Nuclear Reactor)

At the Research Laboratory of Nuclear Reactor, Tokyo Institute of Technology, N.Yamamuro and his collaborators have measured the cross sections of the Sb(n,2n) and Zr(n,2n) reactions in the energy range of 13 - 15 MeV by means of the activation method.

Their programmes in progress are the measurements of the elastic and inelastic scattering of 14 MeV neutrons by the time-of-flight method, using the Cockcroft-Walton type accelerator and the pulsation system.

V. Kyushu University Group (Department of Nuclear Engg.)

1. Proton Emission Reaction in Zn^{64} Induced by 14 MeV Neutrons*

(I.Fujita)

Proton emission reactions in Zn^{64} induced by 14 MeV neutrons are studied by means of multi-plate camera. The cross sections of (n,p) and (n,np) reactions are measured as 159 ± 27 mb and 221 ± 48 mb respectively. These values are the least ones as compared with the values obtained so far. The cross section of direct process is 51 mb. The nuclear temperatures are 1.16 ± 0.08 MeV and 0.44 ± 0.02 MeV corresponding to (n,p) and (n,np) reactions respectively and are in coincidence with the values obtained by other workers. The value of β obtained from angular distribution by Ericson-Rosen theory increases with the energy of emitted protons and the deviation from isotropy is greater for the protons of lower energy. It seems to be inconsistent with the proposal by Allan and Bodansky that anisotropy is due to the emission of secondary protons. From the value of β, the moment of inertia of Cu^{64} is estimated as 4.0×10^{-48} gr.cm^2, which is consistent with the value derived by Carver et al. The measurements on proton emission reaction in Zn^{66} are now in progress.

---

*) Details are given in the Technology Reports of Kyushu Univ. (in Japanese), 37, 294 (1965).

2. Optical Model Calculation of Transmission Coefficients and Total Cross Sections of Protons for Heavy Nuclei*

(Y.Wakuta, M.Sononda, A.Katase, M.Seki, T.Akiyoshi, I.Fujita and M.Hyakutake)

In order to analyse the experimental data of proton-induced fissions, the transmission coefficients and the total cross sections of U^{238}, Th^{232}, Bi^{209}, Pb^{208} and Au^{197} are calculated for protons of 30 to 90 MeV. ELIESE-1 code prepared by the Japanese Nuclear Data Committee was used in the calculations. The results seem to be satisfactory, being compared with the results by Mani et al., although the experimental data of proton scattering are not available in these nuclei for incident protons in the above mentioned energy region.

3. Time-of-Flight Spectrometer for Fast Neutrons

(A.Yoshimura**, M.Sonoda, A.Katase, Y.Wakuta, M.Seki, T.Akiyoshi, I.Fujita and M.Hyakutake)

A time-of-flight neutron spectrometer using associated particle method has been constructed. A time-to-pulse height converter is of pulse-overlapping type and uses a 6BN6 tube as a gate tube. A detector for associated alpha particles is a thin plastic scintillator viewed by a 6810A photomultiplier and a neutron detector is a 50 mm thick plastic scintillator viewed by a 56AVP photomultiplier. Pulses from the two scintillators are transformed into square pulses and applied to the first and the third grids of the 6BN6 tube of the time to pulse height converter. During the time in which both pulses overlap,

---

*) The results are given in the Technical Reports of Kyushu Univ. (in Japanese), 38, 18 (1965)

**) Present address: Institute for Nuclear Study, Tokyo University

the 6BN6 tube is conducting and a voltage pulse proportional to the overlap time is produced by an integrating circuit in the plate circuit. The time difference up to 50 nsec can be measured and the overall resolution is 1.9 nsec. For 14 MeV neutrons, the ground state and excited states of Q = -4.47, -7.6 and -9.61 MeV of Carbon nucleus are well resolved by the flight-path of 100 cm. Inelastic scattering of 14 MeV neutrons by light nuclei (Li, Be and C) and heavy nuclei (Au, Tl, Pb and Bi) are now under investigation.

4. Energetics of Fissions Induced by 55 MeV Protons*

(M.Sonoda, A.Katase, Y.Wakuta, M.Seki, A.Yoshimura, T.Akiyoshi, I.Fujita and S.Usami**)

Coincident kinetic energy spectra of fragments in fissions of Bi^{209}, Th^{232} and U^{238} induced by 55.3 MeV protons are measured by back-to-back solid state detector system and contour diagrams of fragment kinetic energy are obtained. From the contour diagrams, total kinetic energy distribution, average total kinetic energy and distance between charge centers of fragments as functions of fragment mass, and initial fragment mass distribution are derived. The results for $Bi^{209}(p,f)$ and $U^{238}(p,f)$ have the similar features as those for $Pb^{206}(He^3,f)$ and $Th^{232}(He^4,f)$ respectively, which were obtained by LASL and our groups by bombardment with projectiles of 20 to 30 MeV. For $Th^{232}(p,f)$, our value of full width at half maximum of total kinetic energy distribution is greater than that of LASL group, probably because of thicker target we used.

---

*) Some results which have been obtained will be published somewhere.

**) Imaharu Engineering High School, Japan

For Au^{197} and natural Pb, only single kinetic energy spectra are measured, because of small cross sections. The spectra show symmetric distribution similar to that of $Bi^{209}(p,f)$.

5. Fragment Angular Distributions in Fissions of Heavy Nuclei Induced by 55 MeV protons *

(M.Sonoda, A.Katase, Y.Wakuta, M.Seki, A.Yoshimura, T.Akiyoshi and I.Fujita)

Angular distributions of fission fragments have been measured with solid state detectors for fissions of U^{238}, Th^{232}, Bi^{209} and Au^{197} induced by 55.3 MeV protons. The measurements were carried out in the backward direction with respect to the incident proton beams. The results were fitted by least-squares method with Legendre polynomials and also compared with the Halpern-Strutinski theory. The $W(0^\circ)/W(90^\circ)$ ratios of U^{238}, Th^{232}, Bi^{209}, and Au^{197} are 1.21 ± 0.02, 1.14 ± 0.03, 1.03 ± 0.07 and 1.04 ± 0.06 respectively. The observed anisotropies for U^{238} and Th^{232} are compared with the results obtained so far.

6. Symmetric and Asymmetric Fission of U^{238} Induced by Helium Ions **

(M.Seki)

The energetics of helium-ion-induced fission of U^{238} has been investigated, a back-to-back solid state detector system being used. The measurements have been made at two center-of-mass angles 90°

---

*) Some of the results obtained will be published somewhere.

**) A detailed description of this work is given in the Journal of the Physical Society of Japan, 20, 190 (1965)

and 160° and at bombarding energies of 27.8, 30.4, 32.6, 34.2 and 35.6 MeV. It is found that the position of the asymmetric fission peak in the kinetic energy contour diagram and the most probable values of E_L, E_H and E_K are nearly independent of the excitation energy of compound nucleus. From the comparison with results obtained so far at lower energies, it is probably concluded that the average total kinetic energy in symmetric fission increases with the excitation energy of fissioning nucleus but the one at the peak in the mass yield distribution is approximately independent of the excitation energy. Some systematics are derived for the average total kinetic energies. The average excitation energy of fragments remains nearly constant in symmetric fission but not in asymmetric fission as the excitation energy of fissioning nucleus increases. The anisotropies for symmetric and asymmetric fission are probably consistent with a theoretical prediction.

7. Fissions of Heavy Nuclei Induced by High Energy Photons*

(M.Sonoda, A.Katase, Y.Wakuta, M.Seki, A.Yoshimura, T.Akiyoshi, I.Fujita and S.Yamawaki)

Kinetic energy spectra and angular distributions of fission fragments for $U^{238}(\gamma,f)$ were measured with solid state detectors in the photon energy range of 200 ~730 MeV. Cross sections for photofission of U, Th, Bi, Pb, Tl and Au were measured with nuclear emulsions. Both types of detectors distinguished well the fission fragments from background. Nuclear emulsions are now being scanned. The results obtained were thus only those with solid state detectors.

---

*) Some of the results will be published somewhere.

The angular distribution of fission fragments from U(γ,f) is nearly isotropic at lower maximum photon energies except the one at 200 MeV, but it becomes anisotropic and has a minimum at about 90° as the maximum photon energy increases. Measured cross sections are in accordance with results obtained by Jungerman and Steiner at lower maximum photon energies, but they are somewhat larger than the values obtained so far at higher energies. The excitation curve as a function of photon energy shows a peak at 380 MeV, which seems to correspond to a peak of the excitation curve for photo-meson production from a nucleon. There are other two peaks at 530 and 650 MeV, but these are not definite. Kinetic energy spectrum of fission fragments for a maximum photon energy shows two peaks. The kinetic energies of these two peaks are nearly constant for the measured range of maximum photon energy. The kinetic energy spectrum for a photon energy which is obtained by simple photon difference method has a symmetric distribution with a single peak.

Note: The above experiments of Nos. 4, 5, 6 and 7 were made using a F.M.-cyclotron or an electron-synchrotron at the Institute for Nuclear Study, University of Tokyo, Tanashi, Tokyo.

VI. Rikkyo (St. Paul's) University Group

1. Pulse-Height Defects in Semiconductor Detectors for Fission Fragments*

(S.Shirato)

Measurements have been done of the response of surface-barrier detectors to fission fragments as a function of the bias voltage applied to the detectors. It is found that the reciprocal of pulse height decreases linearly with decrease of the reciprocal of average electric field strength within the depletion region. In accordance with such saturation characteristics, the pulse height defect for the fission fragments is shown to decrease approximately linearly with decrease of the reciprocal of the electric field. By extrapolation of the linear relation to the infinite field strength, the pulse height defect for each group of light and heavy fragments is separated into field-dependent and field-independent components. The defect obtained at a finite field strength is a few MeV greater for heavy fragments than for light ones, and this difference comes mainly from the field-independent component. The field-independent defect seems to be smaller than the ionization defect in gas. Possible causes of the pulse height defect are discussed.

---

*) A detailed work is given in the Japanese Journal of Applied Physics 3, 326 (1964).

2. Fission of Uranium-238 Induced by 55 MeV Protons*

(S.Shirato, S.Kubota, H.Takahashi, T.Doke, I.Ogawa, M.Tsukuda and E.Tajima)

Distributions of fragment kinetic energies and masses in the 55 MeV proton-induced fission of U^{238} have been measured in various directions with respect to the beam by using a back-to-back arrangement of surface-barrier detectors. The observed energy distribution showed a single broad peak with a slight shoulder on the high energy side. This indicates a marked growth of symmetric fission. The most probable value of the total fragment kinetic energy was observed to be 156 ± 5 MeV. The initial total kinetic energy before neutron emission was estimated from the value to be about 161 MeV. The mass distribution obtained in the transverse direction was in fair agreement with the radiochemical result. By making a fine comparison between these results, an attempt was made to obtain some information about neutron yields from individual fragments. The mass distribution in the backward direction was almost the same in shape as in the transverse direction, when corrected for the projectile momentum. Furthermore, the observed angular distribution of the composite fragments was less anisotropic than expected from the Halpern-Strutinski theory.

---

*) This work was carried out by use of a F.M.-cyclotron at the Institute for Nuclear Study, University of Tokyo, and details are given in the Journal of the Physical Society of Japan, 19, 1809 (1964).

3. Alpha Decay of Gadolinium-150*

(I.Ogawa, T.Doke, M.Miyajima and A.Nakamoto)

The alpha particle energy and the half-life of Gd^{150} have been measured with a double-grid ionization chamber. Backgrounds are minimized by the grid-collector coincidence technique. The alpha particle energy is determined as 2.715 ± 0.018 MeV by referring to that of Sm^{147} (E_α = 2.23 ± 0.02 MeV) reported by Macfarlane. The half-life is estimated to be (1.4 ± 0.4) x 10^6 yr from the observed counting rate and the total number of Gd^{150} nuclei contained in the specimen. The number is estimated from the observed bata-decay rate of the parent nuclei, Eu^{150}, which are produced by a photo-nuclear reaction Eu^{151} $(\gamma,n)Eu^{150}$. The experimental half-life thus obtained agrees within a factor of 4.4 with the theoretical half-life calculated from the observed alpha-particle energy of the basis of a conventional barrier-penetration theory. The results show that Gd^{150} behaves quite normally in the systematics of rare-earth alpha-decay.

---

*) To be published in the Nuclear Physics.

4. Fission Fragment Energy Spectrum after Prompt Neutron Emission

(H.Kobayashi, A.Nakamoto and M.Hosoe)

The Institute for the Atomic Energy, St. Paul's University, Yokosuka

(J. Phys. Soc. Japan 20 (1965) 176~177, Short Note)

The fission fragment energy spectrum after prompt neutron emission was obtained from the initial spectrum (before neutron emission), being corrected for the energy loss due to the prompt neutron emission.

Instead of using the distribution of neutron energy loss for respective fragment energy E, we used for simplification a mean value $\overline{\Delta E_n}(E)$ only as a function of E. The mean value was calculated from the expression $\langle \Phi(M,E) \cdot \Delta E_n(M,E) \rangle_M$. The fragment energy-energy correlation distribution $W(E_1, E_2)$ was measured. And the mass-energy distribution of fragment $\Phi(M,E)$ was calculated from this distribution. To obtain $\Delta E_n(M,E)$, the following two assumptions were made: (1) The energy loss $\Delta E_n(M,E)$ can be approximated by the relation $(\nu/M) \cdot E$, where ν is prompt neutron number per fission event. (2) The value of ν is independent of its fragment energy, but dependent on the fragment mass. The function $\bar{\nu}(M)$ -- the dependence of ν on the fragment mass -- was read from J. Terrell's results[1].

Our experiment was made on thermal neutron induced fission of U-235. The outputs from two surface barrier Si-Au detectors placed in face-to-face arrangement, supplied the necessary information of the correlation distribution $W(E_1, E_2)$. Energy calibration for the two detectors was made by comparing the measured average pulse heights of the light and the heavy fragment groups with the respective values obtained by the time-of-flight method[2]. The initial mass distribution deduced from $\Phi(M,E)$ was compared with the mass distribution obtained by the time-of-flight method,[3] and is shown in

Fig. 1. Fig. 2 shows the result of $\overline{\Delta E_n}(E)$ obtained by our method. Fig. 3 shows the fragment energy spectrum after neutron emission, and the initial energy spectrum obtained by the time-of-flight method[4] as well.

In the following, some errors caussed by our approximation are discussed: (1) The neutron number $\overline{\nu}(M)$ was used instead of $\nu(M,E)$ to obtain the emitted neutron number, thus the energy dependence of the neutron emission was neglected. Neglection of the energy dependence is supposed to be the greatest cause of the error, however, the available data was not sufficient to estimate the amount. (2) In the measurement of $\Psi(E_1, E_2)$ the detector was calibrated at only two values — average pulse heights of the light and the heavy fragment groups. This means linear approximation of non-linear pulse height response.[5] However, the maximum error of $\Delta E_n(M,E)$ was estimated to be 10%; and at the point (M,E), Φ was so small that the error for $\overline{\Delta E_n}(E)$ did not exceed few per cents. (3) As neutrons are evaporated isotropically in average, the error caused by the neglected term for neutron recoil in equation $\Delta E_n = (\nu/M) \cdot E$ amounts to only 3 %.

The fragment energy spectrum after neutron emission is an effective tool for the determination of the energy dependence of pulse height defect of fission fragment in semiconductor detectors.[5]

References

1) James Terrell: Phys. Rev. 127 (1962) 880.

2) J.C.D. Milton and J.S. Fraser: Canad. J. Phys. 40 (1962) 1626, Table II.

3) Refer to 2) Fig. 6, p. 1640.

4) Refer to 2) Fig. 21, p. 1652.

5) H. Kobayashi, A. Nakamoto and M. Hosoe: (to be published).

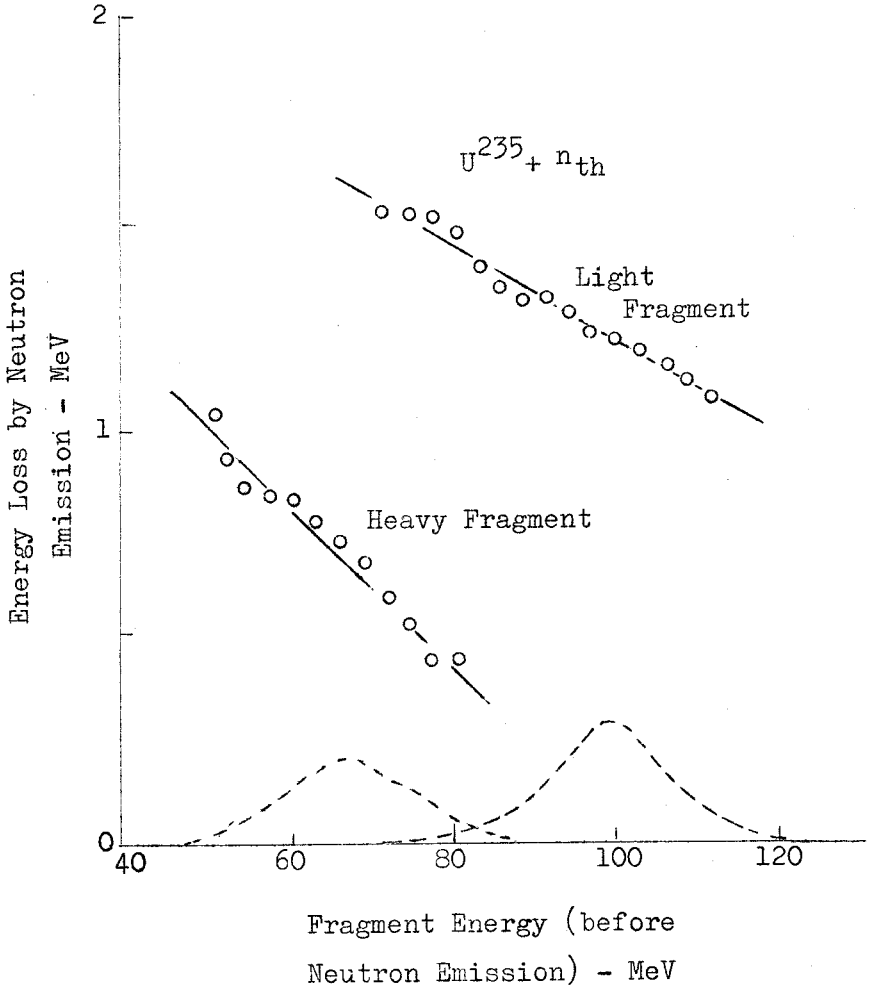

Fig. 2. The average energy loss of the fragment due to the prompt neutron emission vs. fragment energy.

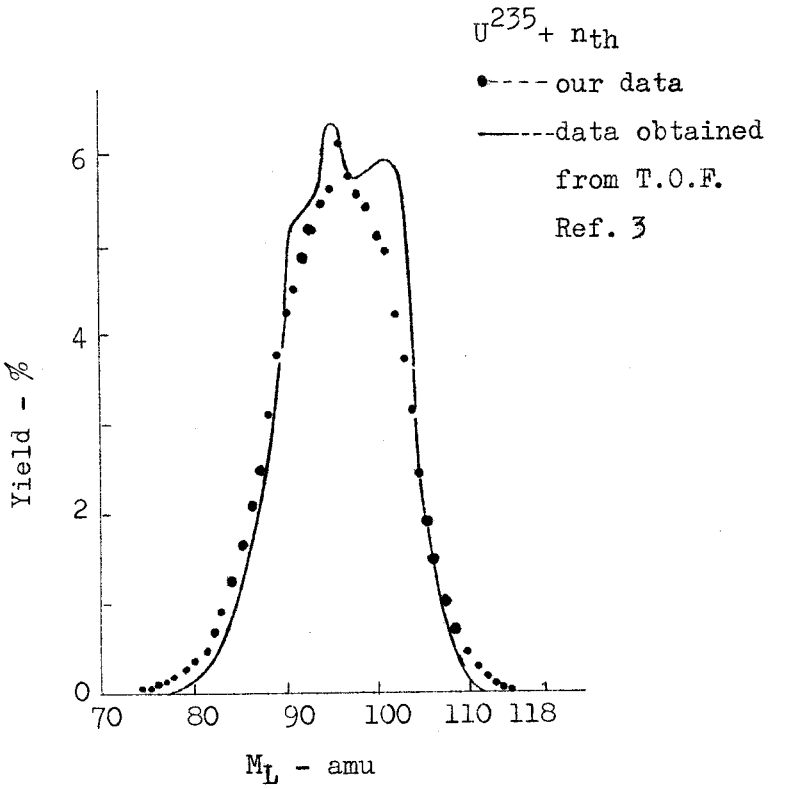

Fig. 1. The initial mass distribution deduced from $\Phi(M,E)$.

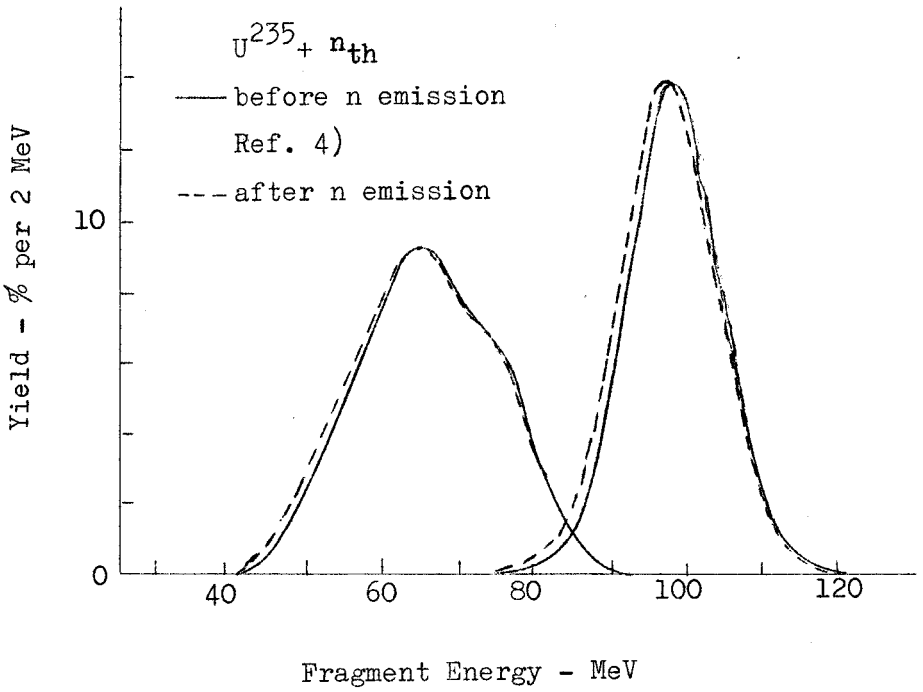

Fig. 3. The fragment energy distributions before and after prompt neutron emission.

VII. Others

Followings are abstracted from papers submitted to the EANDC's International Conference on the Study of Nuclear Structure with Neutrons to be held in Antwerp on July 19 - 23, 1965.

1. Direct (p,n) Reaction in Medium Weight Nuclei

(Y.Saji, Y.Ishizaki, H.Yamaguchi, K.Okano*, B.Saeki**, K.Yuasa** and N.Yoshimura***)

Institute for Nuclear Study, University of Tokyo, Tanashi-machi, Tokyo

The energy spectra and angular distributions (from 5 degree to 80 degree in lab. system) of (p,n) reactions from several medium weight nuclei (^{52}Cr, ^{55}Mn, ^{56}Fe, ^{58}Ni, ^{80}Se, ^{88}Sr, ^{89}Y, ^{90}Zr and ^{94}Zr) have been measured for 14.2 ± 0.05 MeV protons by the time-of-flight method. Many peaks corresponding to the transitions to the isobaric ground states, to the isobaric excited states and to the configuration states have been observed in the neutron spectra and Q-values of those peaks were also determined.

---

* Japan Atomic Energy Research Institute, Tokai

** Department of Physics, Konan University, Kobe

*** Tokyo Shibaura Electric Co., Ltd., Tamagawa, Kawasaki

2. The Li^6 (γ, np) He^4 Reaction

(H.Hirabayashi and Y.Oda)

Department of Physics, Tokyo Institute of Technology, Tokyo

In the study of the photonuclear reactions of Li^6 with relatively low energy γ-rays ($E_{\gamma max}$ = 15.7 MeV), we have found recently a prominent emission of protons of energies smaller than 1.9 MeV. The protons are interpreted to be produced by a resonant absorption of γ-rays at the 8.4 MeV state of Li^6. Here, the transition is of M1 nature. In this case, one expects the emission of intense corresponding neutrons. The inquiry is now under progress for this kind of neutrons.

3. Optical Model Analyses of Elastic and Inelastic Scattering of Neutrons

(K.Nishimura*+, S.Igarashi** and M.Nakamura***)

* Japan Atomic Energy Research Institute, Tokai

** Central Research Laboratory, Hitachi, LTD.
Ozenji, Kawasaki-city, Kanagawa

*** IBM Japan LTD., Nihonbashi, Tokyo

In this report, it is pointed out that a depth of imaginary part of the optical potential for exit channels has a strong dependence on the nuclear level structures. There have been several works investigating a systematic trend of the potential parameters for entrance channel as a function of energy E and mass number A. But, the trend of the parameters for exit channels has not been studied systematically.

+ Present Address: Northwestern University, Evanston, Illinois.

By using our computer code ELIESE - 1, we analysed the excitation functions of the inelastic scattering of low energy neutrons by some medium weight nuclei and estimated the well depth of the imaginary potential for the exit channels. In this computer code, the simple spherical optical model and Hauser-Feshbach model are included to calculate the elastic and the inelastic scattering cross sections for neutrons, protons and alpha particles.
Using this computer code, it is possible to calculate the cross sections by varying the values of the potential parameters with each channel.